

## Precision weak boson production cross-section measurements at LHCb

C. BARSCHEL

*CERN - Geneva, Switzerland*

ricevuto il 20 Giugno 2013; approvato l'1 Luglio 2013

**Summary.** — Precision measurements of weak boson production cross-sections at the Large Hadron Collider (LHC) allow the Standard Model to be tested and parton distribution functions to be constrained. To achieve this goal an absolute precision of 2% or better is desirable on the experimental measurement. We present how such accuracy on the luminosity determination at a hadron collider is achieved in the LHCb experiment. The LHCb measurements are unique in that they combine two methods, the classical van der Meer method and a novel method based on beam-gas interactions. The impact of these precise luminosity measurements on the LHCb analyses of electroweak production measurements are presented.

PACS 13.38.Be – Decays of  $W$  bosons.

PACS 13.38.Dg – Decays of  $Z$  bosons.

### 1. – Introduction

A precision measurement of weak boson production cross-sections provides an important test of the Standard Model and also valuable input to constrain the proton parton density functions (PDFs) [1]. Theoretical predictions of electroweak boson production are known to next-to-next-to-leading-order (NNLO). While these calculations are in good agreement with experiments (see references in [3]), theoretical uncertainties are dominated by the knowledge of the PDFs, and depend on the final state lepton pseudorapidity  $\eta$ .

The LHCb detector [2] is a magnetic dipole forward spectrometer covering the pseudorapidity range  $2 < \eta < 5$ , designed to study flavour physics. This kinematic range permits measurements to be made that provide input to PDFs in the kinematic region  $2 < \eta < 2.5$ , which overlap with ATLAS and CMS, and in the forward region  $\eta > 2.5$  where theoretical prediction have a larger uncertainty and the PDFs are not well constrained by other experiments.

All cross-section measurements require an absolute value of the integrated luminosity as input. A level of luminosity precision of 2% or better is necessary if the cross-section

measurements are not to be dominated by the luminosity accuracy. Three electroweak measurements that are or will be limited by the luminosity uncertainty are presented here. The major electroweak production measurements at LHCb are the muonic decays  $Z \rightarrow \mu\mu$  and  $W \rightarrow \mu\nu$  [3] owing to the highly efficient muon trigger. Additionally, the electron channel  $Z \rightarrow ee$  [4] offers a statistically independent sample with different systematic uncertainties. The three measurements are performed at  $\sqrt{s} = 7$  TeV.

## 2. – Cross-sections measurements

**2.1.  $W$  production using  $W \rightarrow \mu\nu$  decay.** – The  $W$  cross-section is measured in bins of  $\eta^\mu$  and is defined as

$$(1) \quad \sigma_{W \rightarrow \mu\nu}(\eta^\mu) = \frac{\rho N f_{\text{FSR}}}{A \mathcal{L} \epsilon},$$

with  $\rho$  the sample purity,  $N$  the number of candidates,  $A$  the acceptance,  $\mathcal{L}$  the integrated luminosity,  $\epsilon$  the experimental efficiencies and  $f_{\text{FSR}}$  the final-state electromagnetic radiation correction factor. Events are selected using a single muon trigger requiring a high transverse momentum  $p_T > 10$  GeV/ $c$ . The analysis is based on 2010 data with an integrated luminosity of 37 pb $^{-1}$ .  $W$  boson candidate events are required to have a single muon with  $p_T > 20$  GeV/ $c$  and lie within the pseudorapidity range  $2 < \eta < 4.5$ . The  $W^\pm$  purity is about 80% and is determined from a template fit to the  $p_T$  spectra; the signal shape is determined from simulation. The background contributions from decay-in-flight,  $Z \rightarrow \mu\mu$ ,  $\tau$  decays of  $W$  and  $Z$ , and heavy flavour decays are either determined from data or from simulation. A detailed description is provided in ref. [3]. The muon  $p_T$  distribution for the selected  $W$  candidates is shown in fig. 1a. A total of 14660  $W^+$  and 11618  $W^-$  candidates are selected for the analysis.

**2.2.  $Z$  production using  $Z \rightarrow \mu^+\mu^-$  decay.** – The  $Z$  cross-section is measured in bins of  $Z$  boson rapidity  $y$  as function of the two muons in bins  $\eta_i^\mu, \eta_j^\mu$  and is defined as

$$(2) \quad \sigma_{Z \rightarrow \mu\mu}(y) = \frac{\rho f_{\text{FSR}}}{A \mathcal{L}} \sum_{\eta_i^\mu, \eta_j^\mu} \frac{N(\eta_i^\mu, \eta_j^\mu)}{\epsilon(\eta_i^\mu, \eta_j^\mu)},$$

with  $N(\eta_i^\mu, \eta_j^\mu)$  the number of  $Z$  candidates in the corresponding  $y$  bin,  $\epsilon(\eta_i^\mu, \eta_j^\mu)$  the efficiency of the reconstructed muons,  $A$  the acceptance,  $\mathcal{L}$  the integrated luminosity, and  $f_{\text{FSR}}$  the final-state radiation correction. The  $Z \rightarrow \mu^+\mu^-$  analysis uses the same trigger requirement and integrated luminosity as  $W \rightarrow \mu\nu$ .  $Z$  boson candidates are selected by requiring two muons having a combined invariant mass  $M_{\mu\mu}$  within  $60 \leq M_{\mu\mu} \leq 120$  GeV/ $c^2$  that lie in the pseudorapidity range  $2 < \eta < 4.5$  and have a  $p_T$  above 20 GeV/ $c$ . A total of 1966  $Z$  candidates are selected. The background contribution from  $Z \rightarrow \tau\tau$  decay where both taus decay to muons is estimated from simulation. Contributions from heavy flavour  $b\bar{b}$  and  $c\bar{c}$  decays are determined from data. The invariant mass distribution of the  $Z$  candidates is shown in fig. 1b.

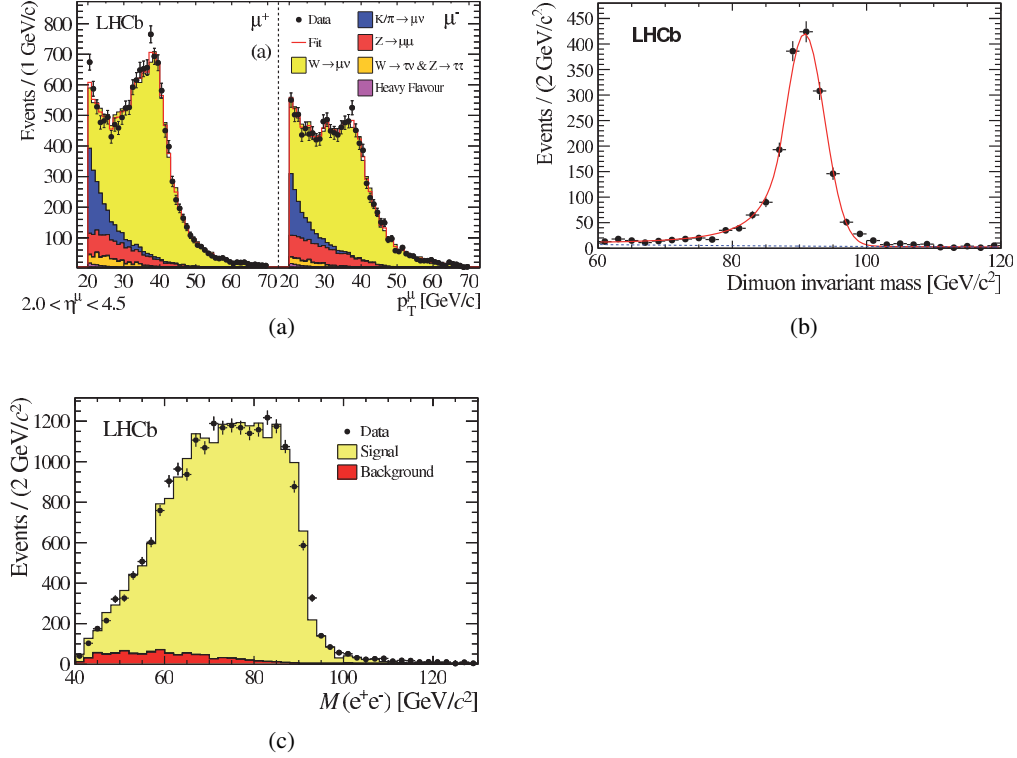


Fig. 1. – (a) Distribution of muon  $p_T$  for W candidates; (left) for  $\mu^+$ , (right) for  $\mu^-$ . The estimated background contributions are labelled in the legend. (b) Invariant mass distribution of  $Z \rightarrow \mu^+\mu^-$  candidates. The fit shown to the reconstructed data points is a Crystal Ball [5] plus exponential function. (c) Invariant mass distribution of  $Z \rightarrow e^+e^-$  candidates.

**2.3. Z production using  $Z \rightarrow e^+e^-$  decay.** – The Z cross-section is measured in bins of Z boson rapidity  $y$  and also in bins of  $\phi^*$ <sup>(1)</sup> is defined as

$$(3) \quad \sigma_{Z \rightarrow e^+e^-} = \frac{\rho N(e^+e^-)}{\epsilon \mathcal{L}} \cdot f_{\text{FSR}},$$

with  $N(e^+e^-)$  the number of Z candidates,  $\rho$  the sample purity,  $\epsilon$  the combined experimental efficiencies,  $\mathcal{L}$  the integrated luminosity, and  $f_{\text{FSR}}$  the final-state radiation correction. The  $Z \rightarrow e^+e^-$  cross-section measurement is based on a 2011 dataset corresponding to an integrated luminosity of  $0.94 \text{ fb}^{-1}$ . Both electrons are required to have  $p_T > 20 \text{ GeV}/c$  and lie in the pseudorapidity range  $2 < \eta < 4.5$ , additionally the invariant mass of the  $e^+e^-$  pair must be greater than  $40 \text{ GeV}/c^2$ . Electron momentum, rather than energy, is used to reconstruct the invariant mass due to saturation of the LHCb electromagnetic calorimeter readout. As fig. 1c shows, the resultant mass peak

<sup>(1)</sup> The variable  $\phi^*$  is related to the Z boson  $p_T$  but depends only on the angles of the final state particle tracks in the detector, see details in ref. [4].

TABLE I. – *Cross-section results. The first uncertainty is statistical, the second systematic and the third is due to the luminosity measurement.*

Channel	Integrated luminosity	Cross-section
$\sigma_{W^+ \rightarrow \mu^+ \nu}$	$37.5 \text{ pb}^{-1}$	$831 \pm 9 \pm 27 \pm 29 \text{ pb}$
$\sigma_{W^- \rightarrow \mu^- \bar{\nu}}$	$37.5 \text{ pb}^{-1}$	$656 \pm 8 \pm 19 \pm 23 \text{ pb}$
$\sigma_{Z \rightarrow \mu\mu}$	$37.5 \text{ pb}^{-1}$	$76.7 \pm 1.7 \pm 3.3 \pm 2.7 \text{ pb}$
$\sigma_{Z \rightarrow ee}$	$0.94 \text{ fb}^{-1}$	$76.0 \pm 0.8 \pm 2.0 \pm 2.6 \text{ pb}$

is broadened due to bremsstrahlung losses. The major background contribution comes from hadrons showering early in the electromagnetic calorimeter which are misidentified as electrons. This contribution is estimated from data using same-sign  $e^\pm e^\pm$ . Further smaller background contributions from the decays  $Z \rightarrow \tau\tau$  and  $t\bar{t}$  are estimated from simulation.

**2.4. Results.** – Cross-section results are presented in table I. All measurement uncertainties are dominated by either the systematic uncertainty or by the uncertainty in the luminosity measurement. In most cases the systematic uncertainty is dominated by the limited number of events available to determine the background and efficiency, and will be reduced when using more data. However, the luminosity uncertainty has different sources, as discussed in the next section.

### 3. – Luminosity measurements

In a circular collider, the instantaneous luminosity for one pair of relativistic colliding bunches is given by [6]

$$(4) \quad L = f N_1 N_2 \int \rho_1(x, y, z, t) \rho_2(x, y, z, t) dx dy dz dt,$$

with  $N_1 N_2$  the bunch population product,  $f$  the revolution frequency (11245 Hz at the LHC) and  $\rho_1, \rho_2$  the particle densities of both bunches. The subscripts 1,2 indicate the two beams. The integral part in (4) is called the overlap integral and is measured in dedicated experiments using two independent methods. The first method, the “van der Meer” scan method, measures the overlap integral by scanning the beams across each other in the vertical and horizontal plane. The second method, “beam-gas imaging”, which is unique to LHCb, measures the single beam transverse shapes using beam-gas interactions vertices; both methods are described in detail in ref. [7].

The present integrated luminosity uncertainty of 3.5%, based on 2010 data, is dominated by the beam intensity measurement and by the low beam-gas rate which limits the ability to precisely measure the bunch shape and evaluate the vertex resolution. The uncertainty on the beam intensity, which is provided by LHC instrumentation, has been reduced since 2011 and now typically accounts for less than 0.5% in most cases.

The LHCb experiment uses a neon gas injection system since 2012 to increase the gas pressure at the interaction point during dedicated luminosity measurements; the pressure is raised by a factor of about 100. The increased statistics accumulated over 10 to 20

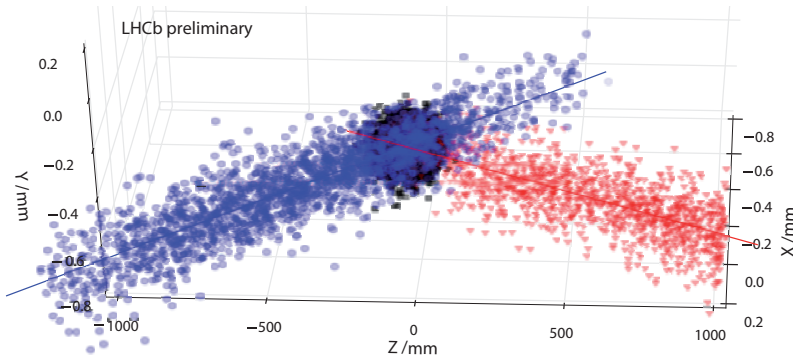


Fig. 2. – Three-dimensional view of beam-gas vertices. The blue circles on the left are from beam1-gas, the red triangles on the right are from beam2-gas and black squares in the center are  $pp$  interactions. The effect of the crossing angle in the horizontal plane is visible.

minutes permit a full three-dimensional image of the beams (as shown in fig. 2) to be reconstructed and the single beam shapes, position and angles required to evaluate the overlap integral, to be measured.

Vertex positions measured with the main LHCb silicon tracking detector (VELO) have an accuracy ranging from  $10\ \mu\text{m}$  to  $50\ \mu\text{m}$  depending on the vertex  $z$  position along the beam axis, the number of reconstructed tracks, and whether the vertex originated from a beam-beam or beam-gas interaction. The vertex resolution is therefore measured and parametrized independently for beam-beam interactions and beam-gas interaction for both beams as a function of track multiplicity,  $z$  position and transverse axis. Resolution parametrization results for beam-beam interactions are shown in fig. 3a.

Single beam profiles are measured by fitting the vertex distributions after deconvolving the VELO resolution, taking the beam directions and positions into account. An example of such a resolution unfolding is shown in fig. 3b. The resolution deconvolution is performed simultaneously on 3 different  $z$  regions per beam.

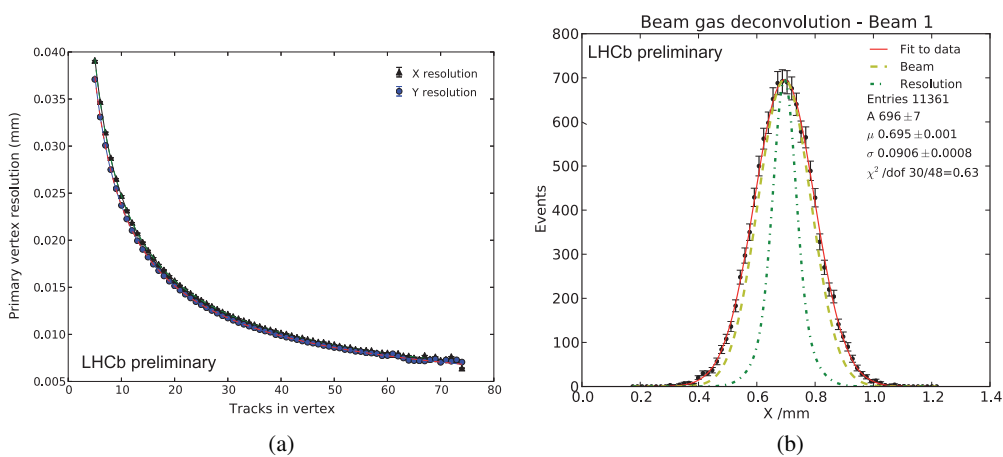


Fig. 3. – (a) Vertex resolution for  $pp$  interactions as a function of the number of tracks. (b) Example of resolution deconvolution measuring the transverse profile of beam 1 in the  $x$  coordinate.

All beam shape parameters are measured simultaneously for both beams in a global fit using a double Gaussian profile per transverse axis. The luminous region shape and position is fully predicted by single beam parameters and is included in the global fit to further constrain the fit parameters. The statistical uncertainty on the overlap integral per bunch pair and 20 minutes integration time is typically less than 0.5%. The main challenge of beam-gas imaging arises from the understanding of the vertex resolution and correlations between the transverse axes. Nevertheless, improvements on resolution measurements and larger number of interactions gained with gas injection will allow LHCb to reach an absolute uncertainty of about 2% with the beam-gas method alone.

#### 4. – Summary

New luminosity measurements performed in 2012 and in particular the beam-gas imaging method using gas injection will provide a relative luminosity uncertainty close to or below 2%. Furthermore, beam-gas results will be combined with the classical van der Meer method; this unique capability of LHCb to combine two independent luminosity measurements will ensure an accuracy below 2%. While present electroweak cross-section measurements are limited by the luminosity uncertainty, new analyses based on 2012 data will not only profit from about twice more data, but also from a significantly higher precision of the luminosity measurement.

#### REFERENCES

- [1] THORNE R. S. *et al.*, arXiv:0808.1847 (2008); doi:10.3360/dis.2008.30.
- [2] ALVES A. A. jr. *et al.* (LHCb COLLABORATION), *JINST*, **3** (2008) 08005.
- [3] AAIJ R. *et al.* (LHCb COLLABORATION), *JHEP*, **06** (2012) 058.
- [4] AAIJ R. *et al.* (LHCb COLLABORATION), *JHEP*, **02** (2013) 106.
- [5] SKWARNICKI T., PhD thesis (Institute of Nuclear Physics) 1986, Krakow DESY-F31-86-02.
- [6] NAPOLY O., *Part. Accel.*, **40** (1993) 181.
- [7] AAIJ R. *et al.* (LHCb COLLABORATION), *JINST*, **7** (2012) 01010.